

Borel Summation Of Asymptotic Series In Dynamics Of Fluid Flows. Diffusion Versus Bifurcations

D. Volchenkov *and R. Lima

*Centre de Physique Thorique (CPT), CNRS Luminy Case 907,
13288 Marseille Cedex 9, France*

E-Mails: volchen@cpt.univ-mrs.fr, lima@cpt.univ-mrs.fr

September 21, 2018

Abstract

The Brownian motion over the space of fluid velocity configurations driven by the hydrodynamical equations is considered. The Green function is computed in the form of an asymptotic series close to the standard diffusion kernel. The high order asymptotic coefficients are studied. Similarly to the models of quantum field theory, the asymptotic contributions demonstrate the factorial growth and are summated by means of Borel's procedure. The resulting corrected diffusion spectrum has a closed analytical form. The approach provides a possible ground for the optimization of existing numerical simulation algorithms and can be used in purpose of analysis of other asymptotic series in turbulence.

PACS codes: 47.10.ad, 47.27.E-, 47.27.ef

Keywords: Brownian motion, Asymptotic series, Borel summation, Simulation on fluid flows

*The Alexander von Humboldt Research Fellow at the BiBoS Research Center

1 Introduction

Theoretical investigations of two dimensional (2D) cross-field transports in the operating ITER-FEAT calls for an increasing confidence in the modelling efforts that force one to search for the new principles of simulations.

It has been reported [1, 2] that the solutions of forced dynamical equations describing the fluid flows (such as the 3D Fourier transformed Navier-Stokes (FNS) equation, the Burgers equation, *etc.*) may be represented, point wise, as the expected values of a branching random walk process statistic. The statistic samples the Fourier transforms of both the initial data and the forcing at various random frequencies as directed by the leaves of the binary branching process, and then combines the results together, in a multiplicative way, according to the binary bifurcation nodes of the process. The branching random walk holds in state $k \geq 1$, $k \in \mathbb{N}$ for an exponential time with parameter νk^2 ($\nu > 0$ is the diffusion coefficient) then it is replaced by no offspring with probability $1/2$, otherwise replaced by two frequencies j and $k - j$, with j picked uniformly over $[1, \dots, k - 1]$. The process is repeated independently for each of the offspring sequences.

The use of finite binary tree algorithms is very plausible since they can be easily implemented and optimized that would drastically improve the effectiveness of large scale simulations on fluid flows. However, it has been discovered that the definition of the stochastic process relevant to the modelling of complicated cross-field transports in plasma is a tough problem. Even if such the branching multiplicative process exists, its fast convergence is questionable. To illustrate the problem, we have performed a preliminary simulation on the FNS. We have tried to reproduce the well-known Kolmogorov's inertial range for the fully developed turbulence in the 3D FNS forced in the small moments (in the large scales). We have sampled the binary trees independently for each of velocity components, but limit the total number of samples just to 250 for each point (k, t) . For the small moments, just a few different binary trees can be constructed and all of them arise in samplings that fits well the fully developed turbulence statistics (see Fig. 1). However the number of different branching trees that could appear in simulations is huge for k large and apparently grows very fast with k . In this case, the set of randomly generated 250 samples obviously does not provide a reliable base for the turbulent statistics that is evident from the excessively strong trembling of data worsening as the momentum k grows up. The data is presented in Fig. 1 in the form of a box plot indicating the scattering. The central point of a box shows the median, the lower line of a box indicates the first quartile, and the upper line shows the third quartile. The whiskers are extended to the maximum and minimum points. Apart from the forced region, an inertial range appears for any nontrivial

initial condition. The strong data scattering in the region of large moments indicates that the number of samples should be essentially increased. It is important to mention that the classical methods developed in [1] do not provide us with tools for the control of convergence for the stochastic multiplicative branching processes that forces us seriously concerns to the problem.

In the present paper, we propose an alternative method that would optimize the simulations on fluid flows. It is closely related to that of branching Brownian motion and uses the techniques borrowed from the quantum field theory to control the computation accuracy. Applications of field theory methods to the various problems of statistical physics and critical phenomena theory have a long history. Nowadays, they have converted into a powerful tool for the effective studying of stochastic phenomena described by the partial differential and integro-differential equations. The problems of statistical physics, in their turn, had also enriched the field theory methods as well.

We study the Green functions of equations describing the incompressible fluid flows by constructing their functional representations. Our approach is based on the ideas of the MSR formalism (after Martin-Siggia-Rose) treating the classical Langevin equations as a kind of Brownian motion. In such a framework, the stochastic averages with respect to the Gaussian distributed random forces stirring the system can be interpreted as some functional averages (see Sec. 2). It is worth mentioned that they are nontrivial even if the stochastic force is put to zero. This fact allows modifying the initial MSR approach in a way to apply it to the forced dynamical equations in which the external forcing is not random. The Green functions can be computed by means of perturbation theory in the form of Feynman diagram series (Sec. 3).

We have demonstrated that each Feynman graph in the series equals to an average over a forest of multiplicative branching binary trees (of the certain topological structure) implemented in [1] that establishes the direct relation between their methods and the field theory approach that we use (Sec. 3). However, the diagram series converges much faster than the multiplicative branching process since each diagram represents an average of branching process over all allowed configurations of moments. We have demonstrated the advantage of method for the stirred Burgers equation supplied with a periodic boundary condition (Sec. 4). In this simple example, the diagrams can be computed analytically, and the series converges very fast. The Fourier spectrum for the Green function forms the asymptotic series starting from the standard diffusion kernel. Fluctuations arise due to the consequent bifurcations of media resulting in the cascade of consequent partitions of moments, $\mathbf{k} = \mathbf{q} + (\mathbf{k} - \mathbf{q})$. The magnitude of relevant corrections to the diffusion spectrum tends to zero as $t \rightarrow t_0$, and the saddle-points (instanton) analysis can be applied to study the "large order" asymptotic contributions (see Sec. 5). The central point

of method is that a coefficient in the asymptotic series is calculated by the Cauchy integral

$$G^{(N)} = \frac{1}{2\pi i} \oint \frac{dg}{g^{N+1}} \sum_{N=0}^{\infty} g^N G^{(N)} = \frac{1}{2\pi i} \oint \frac{dg}{g} \sum_{N=0}^{\infty} g^N G^{(N)} \exp(-N \log g)$$

where the integration contour encircles $g = 0$ in the complex plane. If the asymptotic series $\sum_N G^{(N)} g^N$ is a functional integral, but N is a large number, one can estimate the large order coefficient $G^{(N)}$ calculating the functional integral by the steepest descent method [3]. The saddle-point equations describing the "equilibrium" state of the hydrodynamical system with respect to the large - order contributions into the Green function can be solved as $t \rightarrow t_0$ when the bifurcations rise the corrections to the pure relaxation dynamics.

The calculations show that the asymptotic coefficients demonstrate the factorial growth like the most of models in quantum field theory. The asymptotic series for the Green function can be summarized by means of the Borel procedure (see Sec. 5). In the limit $t \rightarrow t_0$ the corrections to the diffusion kernel have the closed analytical form.

The proposed approach can be broadly used in the many problems of forced dynamics for the optimization of numerical computations and the analysis of asymptotic series. We conclude in the last section.

2 Stochastic dynamics as the Brownian motion

It is well known that many problems in stochastic dynamics can be treated as a generalized Brownian motion $\langle \delta(u - u(x, t)) \rangle_{\xi}$, in which the classical random field indicating the position of a particle $u(x, t)$ meets a Langevin equation

$$\dot{u}(x, t) = Q(u) + \xi,$$

where ξ is the Gaussian distributed stochastic force characterized by the correlation function $D_{\xi} = \langle \xi \xi \rangle$. Here the angular brackets $\langle \dots \rangle_{\xi}$ denote an average position of particle with respect to the statistics of ξ . $Q(u)$ is some nonlinear term which depends on the position $u(x, t)$ and its spatial derivatives. Such a representation was a key idea of the formalism [4].

An elegant way to obtain the field theory representation of stochastic dynamics is given by the functional integral

$$\langle \delta(u - u(x, t)) \rangle_{\xi} \equiv \int D\xi \exp \text{Tr} \left(-\frac{1}{2} \xi D_{\xi} \xi \right) \delta(u - u(x, t)) \quad (1)$$

where the Tr-operation means the integration $\int dx dt$ and the summation over the discrete indices. The instantaneous positions $u(x, t)$ meet the dynamical equation that can be taken

into account by the change of variables

$$\delta(u - u(x, t)) \rightarrow \delta(\dot{u}(x, t) - Q(u) - \xi) \quad (2)$$

should the solution of dynamic equation exists and is unique. The use of integral representation for the δ -function in (1) transforms it into

$$\int D\xi DuDu' \exp \text{Tr} \left(-\frac{1}{2} \xi D_\xi \xi - iu' + u'Q(u) + u'\xi \right) \det M, \quad (3)$$

in which $u'(x, t)$ is the auxiliary field that is not inherent to the original model, but appears since we treat its dynamics as a Brownian motion. The Jacobian $\det M$ relevant to the change of variables (2) is discussed later.

The Gaussian functional integral with respect to the stochastic force ξ in (3) is calculated

$$\int DuDu' \exp(S(u, \eta)) \det M, \quad S(u, u') = \text{Tr} \left[-\frac{1}{2} u' D_\xi u' - u' \dot{u} + u' Q(u) \right]. \quad (4)$$

By means of that all configurations of ξ compatible with the statistics are taken into account. The integral (3) identifies the statistical averages $\langle \dots \rangle_\xi$ with the functional averages of weight $\exp S$. The formal convergence requires the field u to be real and the field u' to be purely imaginary.

The functional averages in (4) can be represented by the standard Feynman diagram series exactly matching (diagram by diagram) the usual diagram series found by the direct iterations of the Langevin equation averaged with respect to the random force. This fact justifies the use of functional integrals in stochastic dynamics at least as a convenient language for the proper diagram expansions.

The Jacobian $\det M$ in (3) depends upon the nonlinearity $Q(u)$. If $Q(u)$ does not depend upon the time derivatives, all diagrams for $\det M$ are the cycles of retarded lines $\overleftarrow{\Delta} \propto \theta(t - t')$ and equal to zero excepting for the very first term,

$$\det M = \text{const} \cdot \exp \text{Tr} \Delta, \quad (5)$$

Following [5], in the paper, we take the convention for the Heaviside function of zero argument, $\theta(0) = 0$, so that $\det M = \text{const}$.

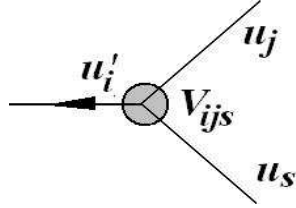
Below, we consider the field theory formulations of equations describing the fluid flows. We suppose that the fluid is incompressible, $\text{div } u = 0$. In the Fourier space, the relevant transversal (rotational) component of u can be allocated by means of the transversal projector,

$$P_\perp(k) = \delta_{ij} - \frac{k_i k_j}{k^2}.$$

The transversal projection of Navier-Stokes equation (NS) lacks of the pressure gradient and the longitudinal component of nonlinear term, $[(u\partial)u]_{\parallel}$. Any solution of it corresponds to some vortex of momentum k . The MSR action functional for the transversal NS is

$$S(u, u') = \text{Tr} \left[-\frac{1}{2} u' D_{\xi} u' - u' \dot{u} + \nu u' \Delta u - u' V(uu) \right] \quad (6)$$

where V is the differential operator $V_{ijs} = i(k_j \delta_{is} + k_s \delta_{ij})/2$ (in the Fourier space). The field theory with the action functional (6) has been discussed in details in [5]. The functional averages computed with respect to the statistical weight $\exp S$ can be expanded into the series of Feynman diagrams drawn with the interaction vertex in which the spatial derivative $V(k)$ is



encircled and the arrow denotes the u' -tail, and two propagators (lines) which have the following analytical representations (in the Fourier space)

$$\Delta_{uu'} = \frac{P_{\perp}}{(-i\omega + \nu k^2)}, \quad \Delta_{uu} = \frac{P_{\perp} D_{\xi}}{(\omega^2 + \nu^2 k^2)} \quad (7)$$

The inverse Fourier transform of $\Delta_{uu'}$ shows that it is retarded, $\Delta_{uu'} \propto \theta(t - t_0)$. Graphs for the Green functions in the theory with the action functional (6) exactly match the well-known diagram expansion of Wyld [6] developed by the direct iterations of stochastically driven NS with respect to its nonlinear term with the consequent averaging over the Gaussian distributed random force.

One can hardly formulate a general method converting a problem of stochastic dynamics into a field theory (there are many, [7]) but once it is done, it allows for applying the powerful techniques within the well controlled approximations.

3 Branching representations to the Green function of Navier-Stokes

Many dynamical systems are driven by the non-random external forces. It is worth to mention that if one assumes $|\xi| \rightarrow 0$ (and consequently $D_{\xi} \rightarrow 0$) in the action functional (6), it is retained, but then the diagram series is trivial since the velocity field propagator vanishes, $\Delta_{uu} = 0$. However, the diagram series would be recovered by means of regular external forcing.

For instance, let us consider the Cauchy problem for the NS equation,

$$\dot{u}_j + \partial_i (u_j u_i) = \nu \Delta u_j + \delta(x - x_0) \delta(t - t_0), \quad (8)$$

supplied with the localized integrable initial condition $u_0 = u(0, x)$ that means the external force $f(x, t) = \delta(x - x_0) \delta(t - t_0)$ acting on the system. The relevant action functional

$$S(u, u') = \text{Tr}[-u' \dot{u} - g\nu u' V(uu) + \nu u' \Delta u] + u'(x_0, t_0) \quad (9)$$

includes the ultra-local interaction term $u'(x_0, t_0)$. To obtain a formal expansion parameter in the perturbation theory for (9), we have inserted the coupling constant $g\nu \equiv 1$ in front of the interaction term. Despite its physical dimension $[g] = -[\nu]$, its conventional dimension would be different. The appearance of ultra-local terms in a field theory had been discussed in [8]. The basic symmetry of (10) is the Galilean invariance,

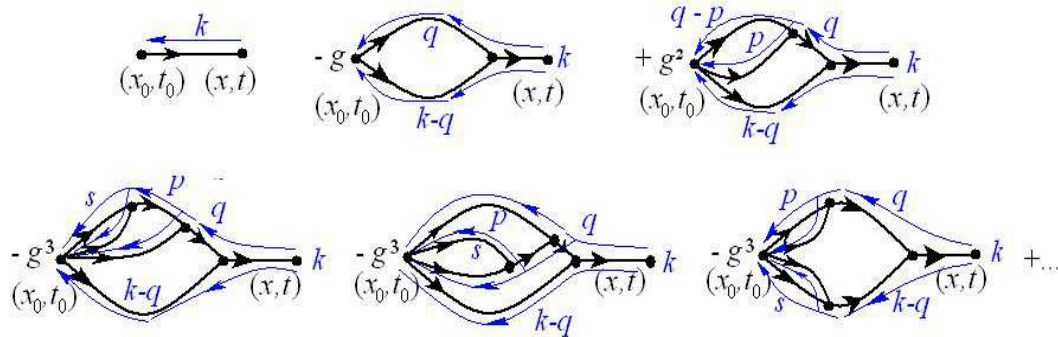
$$u_a(x, t) \rightarrow u(x + X_a(t), t) - a(t), \quad u'(x, t) \rightarrow u'(x + X_a(t), t) \quad (10)$$

where $a(t)$ is an arbitrary function of time decaying rapidly as $|t| \rightarrow \infty$, and $X_a(t) = \int_0^t a(\tau) d\tau$. The transformations (10) define the set of orbits in the configuration space along which the functional averages do not change. It follows that the functional integral itself is proportional to the volume of such orbits. The Green function $G(x, t; x_0, t_0)$ for the Cauchy problem (8) can be computed as the functional average,

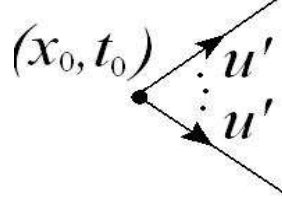
$$G(x, t; x_0, t_0) = \langle u \rangle = \frac{\iint u(x, t) \exp S(u, u') Du Du'}{\iint \exp(S_0) Du Du'}, \quad S_0 = \text{Tr}[-u' \dot{u} + \nu u' \Delta u], \quad (11)$$

in which S is the action functional (9). The above functional average is interpreted as an infinite diagram series,

$$G(x, t; x_0, t_0) = \quad (12)$$



where the arrows on the bold lines indicate the time direction; the thin arrows display the momentum flux traversing the correspondent branch of a graph. The moments are to be



conserved at each node of any graph. In comparison to the standard Wyld diagrams the graphs sketched in (12) contain the local interaction vertex with any number of u' -tails

that recovers the diagrams even if the only line $\overleftarrow{\Delta}_{uu'}$ is retarded. The similar diagrams have been derived for the problem of nonlinear diffusion [9], however, in contrast to them, each vertex in the diagram series (12) contains the differential operator V . The coupling constant $g \equiv 1/\nu$ plays the role of an expansion parameter, so that any graph has the amplitude factor g^ℓ where ℓ is the number of loops presented in it.

The diagram expansion for the Green function would have a definite physical meaning if it converges. The standard analysis of ultraviolet divergences of graphs is based on the counting of relevant canonical dimensions. Dynamical models have two scales, the time scale T and the length scale L , consequently the physical dimension of any quantity F can be defined as $[F] = L^{-d_F^k} T^{-d_F^\omega}$, in which d_F^k and d_F^ω are the momentum and frequency dimensions of F . In diffusion models, these dimensions are always related to each other since $\partial_t \sim \partial_x^2$ in the diffusion equation that allows us to introduce a combined canonical dimension, $d_F = d_F^\omega + 2d_F^k$. One can check out that each term in (9) is dimensionless if the following relations hold: $d_{u'} = 0$, $d_u = d$, $d_\nu = -2 + 2 \cdot 1 = 0$, and $d_g = 2 - (d + 1)$. The field theory (9) is logarithmic (the conventional dimension of the coupling constant $d_g = 0$) for the Burgers equation ($d = 1$), while in two dimensions $d_g = -1$, and $d_g = -2$ for $d = 3$ (the NS equation). Thus, in the infrared region (small moments, large scales) the diagram series in g define just the corrections to the diffusion kernel as $d \geq 2$. However, in the case of Burgers equation, all diagrams look equally essential in large scales.

The diagrams diverge in the ultraviolet region (large moments, small scales) if their canonical dimension

$$d_\Gamma = -d_u N_u - d_{u'} N_{u'} \geq 0$$

where N_u and $N_{u'}$ are the numbers of corresponding external legs in the graph Γ . For the Green function (11), we have $N_{u'} = 0$ and $N_u = 1$. Therefore, there is no any ultraviolet divergent graph in the diagram series (12). For the first glance, it seems that any graph having no external u -legs ($N_u = 0$) and any number of auxiliary fields u' ($N_{u'} > 0$) should

diverge since $d_{u'} = 0$. However, such a graph is also convergent in small scales because of the derivatives $V(k)$ which are always taken outside the graph onto the external u' -legs that effectively reduces its canonical dimension to $d'_\Gamma = d_\Gamma - N_{u'} < 0$. Therefore, the theory (9) has no ultraviolet divergences and need not to be renormalized.

Each Feynman diagram in (12) series corresponds to a certain gyro-dynamical process contributing into $G(x, t; x_0, t_0)$. For the convenience of readers, we give the parallel interpretation of diagrams in terms of multiplicative branching stochastic processes discussed in [1, 2, 10]. The very first diagram is presents the solution of diffusion equation (in d -dimensional space),

$$\Delta(x - x_0, t - t_0) = \frac{\exp(-(x - x_0)^2/4\nu(t - t_0))}{(4\pi\nu(t - t_0))^{d/2}}. \quad (13)$$

It describes the simple viscous dissipation of a vortex with no bifurcations. The second graph in (12) corresponds to a process of twofold splitting. Under the spatial Fourier transformation, it is equivalent to the following analytic expression:

$$\Gamma_1(\mathbf{k}, t) = -g \int_0^\infty dt' V(\mathbf{k}) \Delta(\mathbf{k}, t - t') \int \frac{d\mathbf{q}}{(2\pi)^d} \Delta(\mathbf{q}, t') u_0(\mathbf{q}) \Delta(\mathbf{k} - \mathbf{q}, t') u_0(\mathbf{k} - \mathbf{q}), \quad (14)$$

where $\Delta(\mathbf{k}, t)$ is the spatial Fourier transform of the diffusion kernel (14) and $u_0(\mathbf{k})$ is the Fourier spectrum of initial condition. It is worth to mention that the diagram expansion for the Green function can be also discussed for the function defined a the finite domain supplied with a periodic boundary condition. In the latter case, it has a discrete set of harmonics, and the integral (14) turns into sums.

The time integration in (14) can be performed easily,

$$\Gamma_1 = -gV(\mathbf{k}) \exp(-\nu k^2(t - t_0)) \int_{\mathbf{q} \cdot \mathbf{k} > q^2} \frac{d\mathbf{q}}{(2\pi)^d} \left[u_0(\mathbf{q}) u_0(\mathbf{k} - \mathbf{q}) \frac{\exp(-2\nu(\mathbf{q} \cdot \mathbf{k} - q^2)t_0)}{2\nu(\mathbf{q} \cdot \mathbf{k} - q^2)} \right]. \quad (15)$$

The singularities in Γ_1 appear at $\mathbf{q} = 0$ and $\mathbf{q} = \mathbf{k}$, when the vortex does not bifurcate. The remaining momentum integral in (15) can be interpreted as an expectation value,

$$\wp_1(\mathbf{k}) = \int_{t_0}^\infty d\tau \int \frac{d\mathbf{q}}{(2\pi)^d} [u_0(\mathbf{q}) u_0(\mathbf{k} - \mathbf{q}) \exp(-2\nu(\mathbf{q} \cdot \mathbf{k} - q^2)\tau)], \quad (16)$$

over the Poisson process of vortex bifurcation at momentum \mathbf{k} . Consider the statistical ensemble of the pitchfork bifurcations (see Fig. 2.a) relevant to the set of possible branching random walks discussed in [1].

For each simple tree, the processes start at the vortex with the fixed momentum $k \geq 1$. The branching random walk holds in state k for an exponential time characterized by the parameter

νk^2 . When clock rings, the vortex bifurcates into two offspring with moments $j \in [1, k - 1]$ and $k - j$. They exist for the exponential times accordingly to their moments and then dissipate (that is figured by the crosses in Fig. 2.a). In accordance to the rules of [1], at each vertex of momentum q which dies, one attaches the initial condition $u_0(q)$. The solutions of the fluid flows equations (defined in a finite domain with periodic L_1 initial data) are the expectations of a multiplicative functional that is constituted by the recursive application of the following rule to each node: $-i$ times the product of the pair of values attached to the corresponding pair of input nodes. Each pitchfork bifurcation tree shown in Fig. 2.a presents one of possible primitive realizations of the recursive multiplicative algorithm from [1]. The analytical expression (14) for the second diagram sums up the contributions coming from all pitchfork trees in the forest shown in Fig. 2.

The two-loop diagram in (12) represents the forest of multiplicative branching random walks with the double pitchfork bifurcations schematically shown on Fig.2.b. The graph corresponds to the following analytical expression:

$$g^2 V(\mathbf{k}) \exp(-\nu k^2 (t - t_0)) \times \wp_2(\mathbf{k}) \quad (17)$$

where the functional

$$\wp_2(\mathbf{k}) = \int_{t_0}^{\infty} dt' \int \frac{d\mathbf{p}}{(2\pi)^d} u_0(\mathbf{k} - \mathbf{p}) V(\mathbf{p}) \wp_1(\mathbf{p}) \exp(-2\nu(\mathbf{p} \cdot \mathbf{k} - p^2) t')$$

and $\wp_1(\mathbf{k})$ is defined in (17). The diagrams can be computed provided an integrable initial condition

$$u_0(k) = \sum_m \frac{c_m}{k^m}, \quad (18)$$

is given. In (18), the sum is taken over m odd if the space dimension d is even, and over m even otherwise. For each term in (18), one can compute the functional $\wp_\ell(k)$ of arbitrary order ℓ ,

$$\wp_\ell(k) = \frac{c_m}{(4\pi)^{d\ell/2}} k^{\gamma_\ell} \left[\frac{\Gamma\left(\frac{d}{2} - \frac{m+1}{2}\right)}{\Gamma\left(\frac{m+1}{2}\right)} \right]^{(\ell+1)} \prod_{s=1}^{\ell} \left(\frac{\Gamma\left(\frac{d}{2} - \frac{\gamma_s}{2}\right)}{\Gamma\left(\frac{\gamma_s}{2}\right)} \frac{\Gamma\left(\frac{\gamma_s+m+1-d}{2}\right)}{\Gamma\left(d - \frac{\gamma_s+m+1}{2}\right)} \right), \quad (19)$$

where $\gamma_\ell = \ell d - (\ell + 1)(m + 1)$. Accounting for several terms in (18) makes the analytical computations very difficult, nevertheless they can be performed numerically.

4 One-dimensional diffusion with bifurcations

In the present section we study the correction to the 1D diffusion spectrum arisen due to the Poisson stochastic process of momentum bifurcations. For the sake of simplicity, we consider

the one dimensional diffusion problem supplied with the initial condition in the form of an infinite power series,

$$u_0(k) = \sum_m k^{-m}, k > 0 \quad (20)$$

that corresponds to the function $u_0(x) = -\sin(x)/2$ in the real space. The k -spectrum of the unperturbed diffusion kernel at $t = 5$, $\nu = 0.005$ is shown by the solid line on Fig. 3. The dash line presents the $G(k)$ -spectrum accounting for the corrections due to the pitchfork bifurcations with

$$\wp_1(k) = \frac{1}{4\pi k} (\cos(k) (\text{Ci}(2k) + \text{Ci}(-2k) - \log(-k^2) - 2\log 2 - 2\gamma) + 2\text{Si}(2k) \sin(k)) \quad (21)$$

where $\text{Ci}(k)$ is the cosine integral, $\text{Si}(k)$ is the sine integral, γ is the Euler's constant. The $G(k)$ -spectrum accounting for the corrections due to both the second and the third diagrams in (12) is displayed on Fig. 3 by the dash-dot line. We are not assured that the expansion parameter g is small, and the expansion (12) is the asymptotic series. The fact that the latter spectrums coincide gives us only the indirect evidence in favor of relatively fast convergence rate of diagram contributions in the series. We discuss this problem in more details in the forthcoming section.

Bifurcation of vortexes is the Poisson stochastic process developing with time. On the outlined graphs, we have displayed the exponential decay of G -spectrums at given momentum k . In the real space, the Green function G comprises of several typical patterns of sizes $\propto 1/k_m$ where k_m are the local maximums of the spectrum presented on Fig. 3.

5 The large order asymptotic analysis for the Green function: instanton approach and Borel summation

We have mentioned in the previous section that the expansion parameter g in (12) is not small. To get the information on the convergence of asymptotic series, we study the asymptotic behavior of large order coefficients $G^{(N)}$ in the diagram series

$$G(g) = \sum_{k=1}^N G^{(N)} g^N,$$

as $N \rightarrow \infty$, by the asymptotic calculation of the Cauchy integral,

$$G^{(N)} = \frac{1}{2\pi i} \oint \frac{dg}{g} G(x, t; x_0, t_0) \exp(-N \log g), \quad (22)$$

in which $G(x, t; x_0, t_0)$ is the functional integral (11). The contour of integration in (22) embraces the point $g = 0$ in the complex plain. We compute the functional integral by the steepest

descent method supposing that N is large (instanton method). Instanton approach has been applied to the various problems of stochastic dynamics [11, 12, 13, 14, 15].

Following the traditional instanton analysis, we perform the rescaling of variables in the action functional (9) in order to extract their dependence of N ,

$$u \rightarrow u\sqrt{N}, u' \rightarrow u'\sqrt{N}, g \rightarrow g/N, \nu \rightarrow N\nu, x \rightarrow x\sqrt{N}. \quad (23)$$

This dilatation keeps the action functional (9) unchanged, thus each term acquires the multiplier N and then formally gets the same order, as the $\log g$ in (22). The corresponding Jacobians from the numerator and the denominator of (11) cancel. The saddle point equations are

$$\dot{u}' + g\nu u V(u') + \nu \Delta u' = 0 \quad (24)$$

$$\dot{u} + g\nu V(uu) - \nu \Delta u - \delta(x - x_0) \delta(t - t_0) = 0 \quad (25)$$

$$\nu u' V(uu) = \frac{1}{g} \quad (26)$$

The first equation (24) recovers the original Cauchy problem. The additional equations occur within the framework of our approach since we analyze the dynamics as a kind of Brownian motion. Eq. (25) for the auxiliary field is characterized by the negative viscosity, and therefore $u'(t > t_0) = 0$. The last equation determines the saddle-point value of g that allows to exclude the interaction from the saddle-point equations,

$$\begin{aligned} u' \Lambda u &= -1 + u' \delta(\mathbf{x} - \mathbf{x}_0) \delta(t - t_0), \\ u \Lambda^* u' &= 1, \end{aligned} \quad (27)$$

in which we have introduced the diffusion kernel $\Lambda = \partial_t + \nu k^2$, and its complex conjugate (in the Fourier space) $\Lambda^* = \partial_t - \nu k^2$. It is interesting to note that the possible solutions of (27) should meet the anti-commutation relation,

$$u' \Lambda u + u \Lambda^* u' = u'(x_0, t_0) \delta(\mathbf{x} - \mathbf{x}_0) \delta(t - t_0).$$

Bifurcations of vortexes arisen due to the nonlinearity of hydrodynamic equations do not conclude into a critical regime in the model (9), and therefore the time spectrum in the nonlinear model is the same as for the free diffusion equations, $T \sim L^2$, that is the reason for the branching process to be Poisson distributed with the characteristic time $1/\nu k^2$. One can see that the saddle-point configurations which enjoy (27) should not depend upon the Poisson branching, therefore, the solutions could exist before the bifurcations commence that is as $t \rightarrow t_0$. Taking into account that

$$\delta(x) = \lim_{\varepsilon \rightarrow 0} \frac{\varepsilon}{\pi(x^2 + \varepsilon^2)},$$

one can find that in the limit $t \rightarrow t_0$ (27) is satisfied by the following radially symmetric solutions,

$$u(\mathbf{r}, t) = \sqrt{(\mathbf{r} - \mathbf{r}_0)^2 + (t - t_0)^2}, u'(\mathbf{r}, t) = \frac{\theta(t_0 - t)}{t - t_0} u(\mathbf{r}, t), \quad (28)$$

$$u(\mathbf{r}, t) = \frac{\theta(t - t_0)}{\pi} \arctan\left(\frac{|\mathbf{r} - \mathbf{r}_0|}{2\nu(t - t_0)}\right), u'(\mathbf{r}, t) = -\frac{\pi}{2\nu} \frac{(4\nu^2(t - t_0)^2 + (\mathbf{r} - \mathbf{r}_0)^2)}{|\mathbf{r} - \mathbf{r}_0|}, \quad (29)$$

$$u(\mathbf{r}, t) = \frac{\theta(t - t_0)}{\pi} \arctan\left(\frac{2\nu(t - t_0)}{|\mathbf{r} - \mathbf{r}_0|}\right), u'(\mathbf{r}, t) = \frac{\pi}{2\nu} \frac{(4\nu^2(t - t_0)^2 + (\mathbf{r} - \mathbf{r}_0)^2)}{|\mathbf{r} - \mathbf{r}_0|}, \quad (30)$$

The solutions (28-30) are displayed on Figs. 4-5.

The auxiliary field u' in (28) has a pole at $t = t_0$, and then from (26) it follows that $g_* = 0$ and therefore lays inside the integration contour in (22). In contrast to it, in (30), $u \rightarrow 0$ as $t \rightarrow t_0$ and consequently, $g_* \rightarrow \infty$ that is definitely outside the integration contour. Eq. (29) is a subtle point since $u(r, t = t_0) = \theta(0)/2$, and the position of saddle-point configuration charge g_* depends upon the conventional value $\theta(0)$. While estimating the functional Jacobian in (5), we had assumed that $\theta(0) = 0$. Following such a convention, one can conclude that in this case it is also $g_* \rightarrow \infty$, so that being interested in the large order asymptotic behavior of $G^{(N)}$ we do not need to take the solution (29) into account. Even if one takes $\theta(0)$ as finite, then $0 < g_* < \infty$, and it is always possible to distort the integration contour in such a way to avoid g_* to be encircled. Therefore, (28) is the only solution we need, and below we use

$$g_* \equiv \lim_{\delta t \rightarrow 0} g \simeq \frac{\delta t}{\nu r^2}.$$

Fields u , u' , and the parameter g fluctuate around their saddle-point values u_* , u'_* , and g_* . By means of the standard shift of variables, $u = u_* + \delta u$, $\delta u' = u'_* + \delta u'$, $g = g_* + \delta g$, one makes them fluctuate around zero, so that $\delta u(\infty) = 0$, $\delta u'(\infty) = 0$. Moreover, $\text{Tr } \delta u = \text{Tr } \delta u' = 0$ due to the isotropy of fluid, and therefore these fluctuations are posses the central symmetry, $\delta u = \delta u(r, t)$, $\delta u' = \delta u'(r, t)$, the same as the saddle point configuration.

The contour of integration on the variable δg now passes through the origin point, and is directed there oppositely to the imaginary axis. The integral on δg is conducted now on a rectilinear contour in complex plane ($i\infty, -i\infty$) (in accordance to the standard transformation of a contour in the method of the steepest descent). At the turn of the integration contour $\delta g \rightarrow i\delta g$, the multiplier $(-i)$ appears so the result $G^{(N)}$ is real. The contribution to the Cauchy integral comes from the pole $\delta g = -g_*$ which tends to zero as $t \rightarrow t_0$. The values of functional integrals on the saddle point configurations are proportional to the entire volume of functional integration, they are cancelled in the numerator and denominator simultaneously. While calculating the fluctuation integral, we take into account that the first order contributions

in δu and $\delta u'$ are absent because of the saddle-point condition. We also neglect the high-order interactions between fluctuations, $O(\delta\phi^3)$, $O(\delta\phi^4)$, *etc.* to arrive at the Gaussian functional integral,

$$G^{(N)}(r, \delta t) \simeq_{\delta t \rightarrow 0} \frac{g_*^N N^{N+1/2}}{2\pi} \int \int \mathcal{D}\delta u \mathcal{D}\delta u' \exp -\frac{N}{2} \text{Tr} \left[\delta u' \Lambda \delta u + \delta u \left(\frac{1}{r} \partial_r \right) \delta u \right]. \quad (31)$$

Performing the usual rescaling of fluctuation fields

$$\delta u \rightarrow \delta u / \sqrt{N}, \quad \delta u' \rightarrow \delta u' / \sqrt{N},$$

we compute the Gaussian integral, with respect to δu first, and then the resulting Gaussian integral over $\delta u'$,

$$G^{(N)}(r, \delta t) \simeq_{\delta t \rightarrow 0} N^{N-1/2} \exp(-N \log g_*) \det \Lambda^{-1} \left(1 + O\left(\frac{1}{N}\right) \right). \quad (32)$$

The kernel of operator Λ^{-1} is the Green function of the linear diffusion equation (13). Using the Stirling's formula, one can check that the coefficients $G^{(N)}$ of the asymptotic series (12) demonstrate the factorial grows (like in the most of quantum field theory models):

$$G^{(N)}(r, \delta t) \simeq_{\delta t \rightarrow 0} \frac{N!}{2\pi N} \exp N(1 - \log g_*) \det \Lambda^{-1} \left(1 + O\left(\frac{1}{N}\right) \right). \quad (33)$$

Therefore, the asymptotic series (12) can be summed by means of Borel's procedure. It consists of the following transformation of series (12)

$$\sum_N G^{(N)} g^N = \sum_N \Gamma(N+1) \mathcal{G}^{(N)} g^N = \sum_N \int_0^\infty d\tau \mathcal{G}^{(N)} (g\tau)^N e^{-\tau} \quad (34)$$

where $\mathcal{G}^{(N)} = G^{(N)}/\Gamma(N+1)$ are the new expansion coefficients which do not exhibit the factorial growth. We change the orders of summation and integration in (34) that is indeed incorrect from the mathematical point of view, but is broadly used in physics,

$$\sum_N \int_0^\infty d\tau \mathcal{G}^{(N)} (g\tau)^N e^{-\tau} = \int_0^\infty d\tau e^{-\tau} \sum_N \mathcal{G}^{(N)} (g\tau)^N. \quad (35)$$

We sum over N in the rhs of (35),

$$\frac{\det \Lambda^{-1}}{2\pi} \int_0^\infty d\tau e^{-\tau} \sum_{N=1}^\infty \frac{(g\tau)^N}{N} e^{N(1-\log g_*)} = -\frac{\det \Lambda^{-1}}{2\pi} \int_0^\infty d\tau e^{-\tau} \log \left(1 - \tau \frac{g}{g_*} \right), \quad (36)$$

and integrate it over τ ,

$$G(g) \simeq_{\delta t \rightarrow 0} \det \Lambda^{-1} \left(1 + \frac{1}{2\pi} \text{Ei} \left(\frac{g_*}{g} \right) \exp \left(-\frac{g_*}{g} \right) \right) \quad (37)$$

where $\text{Ei}(x)$ is the exponential integral. The asymptotic diffusion kernels accounting for the corrections due to the bifurcation processes,

$$G(x - x_0, t - t_0) \simeq_{t \rightarrow t_0} \frac{\exp\left(-\frac{(x-x_0)^2}{4\nu(t-t_0)}\right)}{(4\pi\nu(t-t_0))^{d/2}} \left[1 + \frac{1}{2\pi} \text{Ei}\left(\frac{t-t_0}{(x-x_0)^2}\right) \exp\left(-\frac{t-t_0}{(x-x_0)^2}\right) \right], \quad (38)$$

are sketched on Fig. 6. by the dash-dot lines. The unperturbed diffusion kernels are shown by the solid lines.

6 Discussion and Conclusion

In the present paper, we have studied the hydrodynamical flows of incompressible fluids as the Brownian motions over the space of fluid velocity configurations. The essential point of our approach is that we have used the field theory formulation of the dynamics which allowed us for the implementation of various powerful technics borrowed from the quantum field theory. In particular, we have investigated the Green function for the nonlinear hydrodynamical equations.

In the framework of proposed approach, the Green functions can be calculated in the form of well defined asymptotic series. The numerical simulations have demonstrated that these series converge relatively fast. We have studied the high order coefficients of the asymptotic series around the unperturbed diffusion kernel describing the pure relaxation dynamics. We have shown that similarly to the most of quantum field theory models the high order contributions into the Green function exhibit a factorial growth. We have summed over the asymptotic series by means of the standard Borel summation procedure and found the closed analytical form for the corrections (up to an infinite order) to the pure diffusion kernel.

The value of our paper is that it provides a possible ground for the optimization of existing numerical simulation algorithms for the large scale simulations in hydrodynamics. In particular, it can be used in studies of the cross-field turbulent transport in plasmas. Moreover, we have developed the method that can be successfully used in the turbulence studies. It is worth to mention that in the present paper we have constructed the asymptotic solution for the Navier-Stocks equation in the "vicinity" of standard diffusion kernel. However, other asymptotical regimes would also be possible and have to be studied.

7 Acknowledgements

One of the authors (D.V.) is grateful to the Alexander von Humboldt Foundation (Germany) and C.N.R.S. de France, Delegation Provence, for the support that he gratefully acknowledges.

While preparing the paper, D.V. benefited from the hospitality of the Zentrum für Interdisziplinäre Forschung, Universität Bielefeld (Germany).

References

- [1] E. Waymire, R. Bhattacharya, M. Greiner, V.K. Gupta, J.C. Ossiander, E. Thomann, B.M. Troutman, D. Winn: *Lectures on Multiscale and Multiplicative Processes in Fluid Flows*, Instructional and Research Workshop on Multiplicative Processes and Fluid Flows at MaPhySto (2001), University of Aarhus; Bhattacharya, R.N. and Waymire, E.C. (1990): *Stochastic Processes with applications*. Wiley, New York.
- [2] Y. Le Jan and A.S. Sznitman (1997), *Probab. Theory Related Fields* **109**, 343-366.
- [3] J. Zinn-Justin, *Quantum Field Theory and Critical Phenomena*, 3rd Edition, Oxford (1996).
- [4] P. C. Martin, E. D. Siggia, and H. A. Rose, *Phys. Rev. A* **8**, 423 (1973); H. K. Janssen, *Z. Phys. B* **23**, 377 (1976); R. Bausch, H. K. Janssen, and H. Wagner, *Z. Phys. B* **24**, 113 (1976); C. De Dominicis, *J. Phys. (Paris)* **37**, Colloq. C1, C1-247 (1976).
- [5] L. Ts. Adzhemyan, N. V. Antonov, A. N. Vasiliev, *The field theoretic renormalization group in fully developed turbulence*, Gordon and Breach Publ. (1999).
- [6] H. W. Wyld, *Ann. Phys. (NY)* **14**, 143 (1961).
- [7] M. Doi, *J. Phys. A: Math. Gen.* **9**, 1465 (1976); **9**, 1479 (1976); Ya.B. Zel'dovich and A.A. Ovchinnikov, *Zh. Eksp. Teor. Fiz.* **74**, 1588 (1978); P. Grassberger and M. Scheunert, *Fortschr. Phys.* **28**, 547 (1980); L. Peliti, *J. Phys. A: Math. Gen.* **19**, L365 (1986). B. P. Lee, *J. Phys. A: Math. Gen.* **27**, 2633 (1994); J. L. Cardy and U. C. Tuber, *Phys. Rev. Lett.* **77**, 4780 (1996); *J. Stat. Phys.* **90**, 1 (1998).
- [8] K. Symanzik, *Nucl. Phys. B* **190**, 1 (1981).
- [9] N.V. Antonov, J. Honkonen, *Field theoretic renormalization group for a nonlinear diffusion equation*, <http://xxx.lanl.gov:arXiv:nlin.CD/0207006> (2002).
- [10] Ossiander, M.E. and E.C. Waymire (2000): *Statistical estimation theory for multiplicative cascades*. *Ann. Stat.* **28**, 1-21.
- [11] V. Gurarie, A. Migdal (1996), *Phys. Rev. E* **54**, 4908.

- [12] D. Volchenkov, R. Lima (2001), *Phys. Rev. E* **64** (1), 011204-011219.
- [13] A. Yu. Andrianov, M.V. Komarova, M. Yu. Nalimov, *J. Phys. A: Math. Gen.* A/213034/SPE (to published in 2006).
- [14] J. Honkoniemi, M.V. Komarova, M. Yu. Nalimov(2005), *Nucl. Phys. B* 714[FS] 292-306.
- [15] J. Honkoniemi, M.V. Komarova, M. Yu. Nalimov(2005), *Nucl. Phys. B* 707[FS](2005) 493-508.

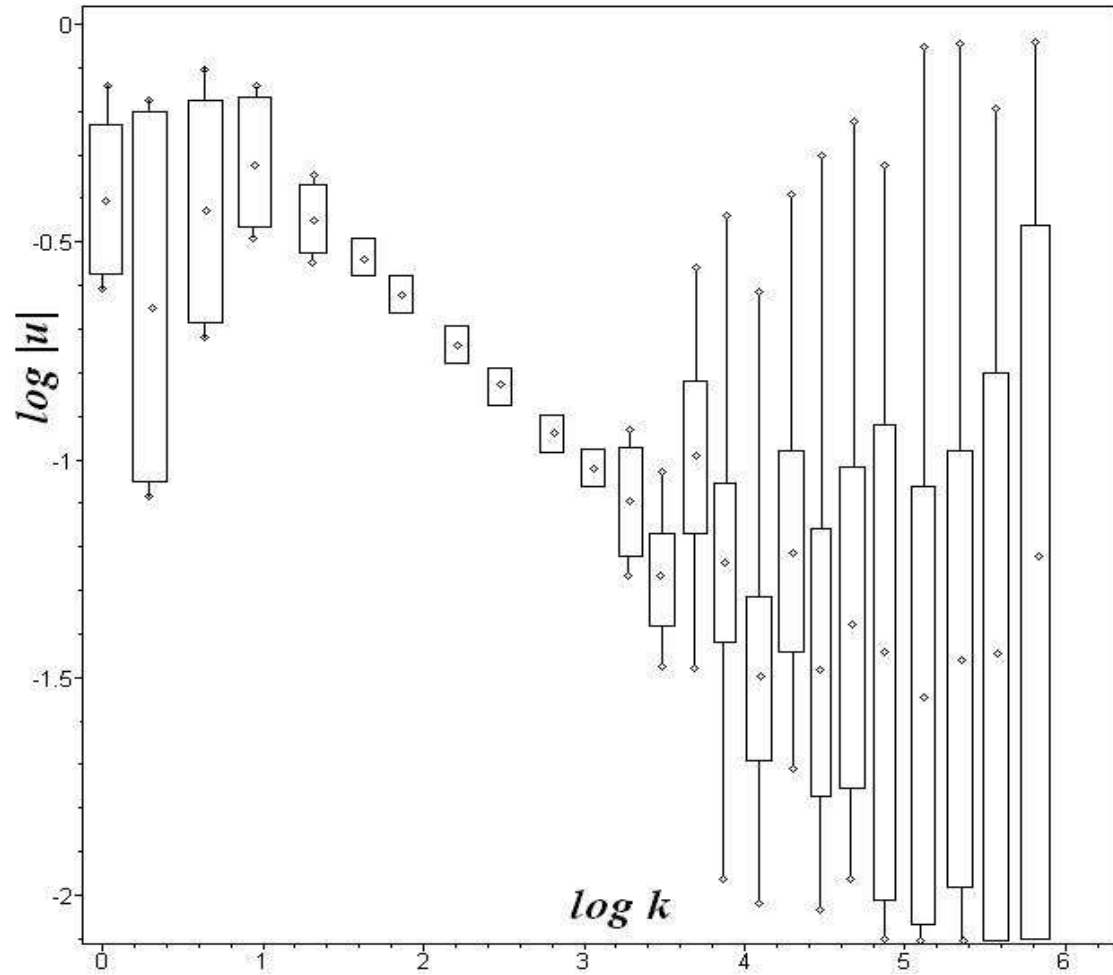


Figure 1: The expectations of the multiplicative binary branching process for the 3D FNS forced in the small moments $k = O(1)$ (in the large scales). The binary trees have been sampled independently for each velocity component, but the total number of samples is limited just to 250 for each point (k, t) . The set of randomly generated 250 samples obviously does not provide a reliable base for the turbulent statistics for the large k that is evident from the excessively strong trembling of data worsening as the momentum k grows up.

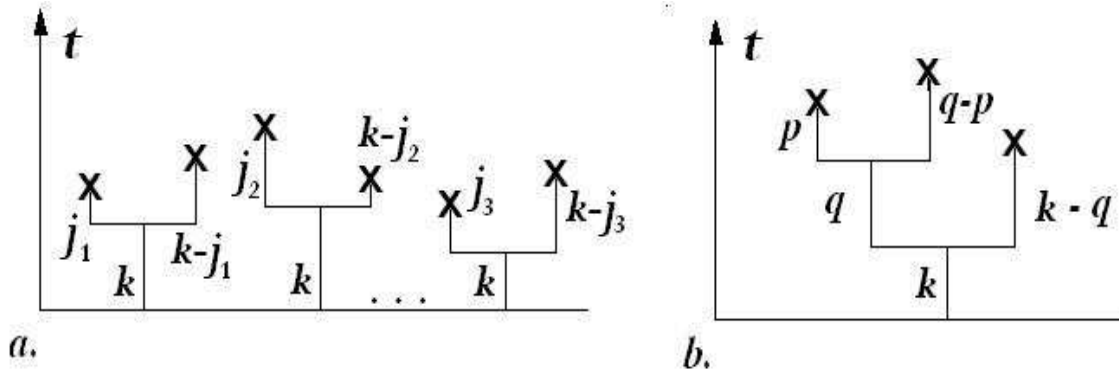


Figure 2: a). The statistical ensemble of the pitchfork bifurcations relevant to the set of possible branching random walks. The branching random walk holds in state k for an exponential time characterized by the parameter νk^2 . When clock rings, the vortex bifurcate into two offspring with moments $j \in [1, k - 1]$ and $k - j$. They exist for the exponential times accordingly to their moments and then dissipate that is figured by the crosses. b). The branching random walks with the double pitchfork bifurcations.

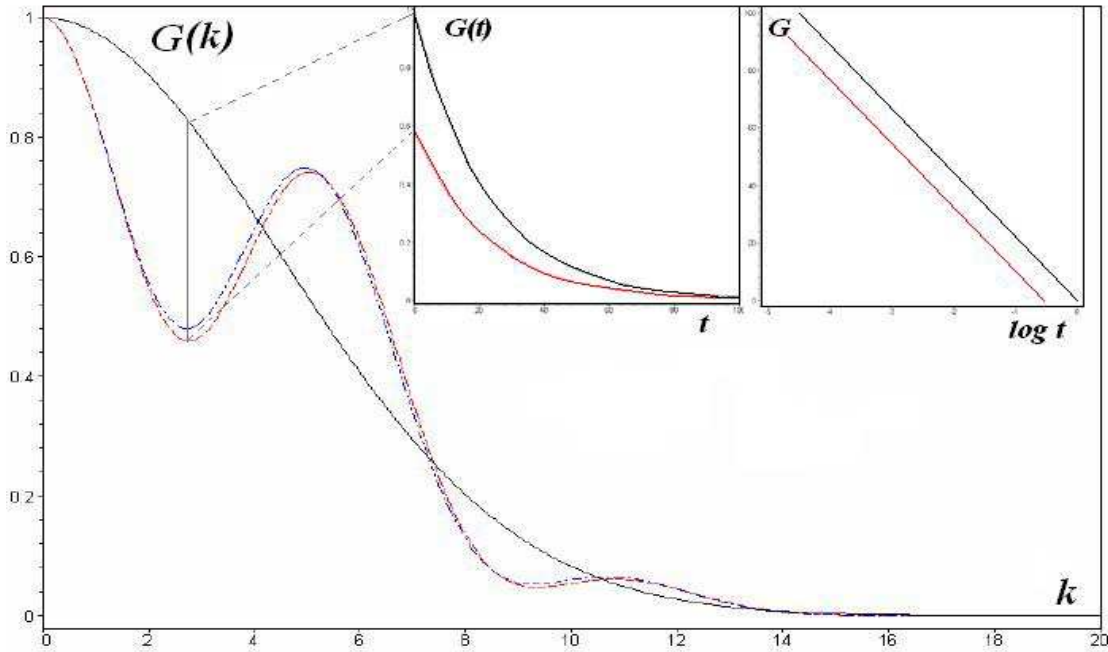


Figure 3: The k -spectrum of the unperturbed 1D diffusion kernel at $t = 5$, $\nu = 0.005$ is shown by the solid line. The dash line presents the $G(k)$ -spectrum accounting for the corrections due to the pitchfork bifurcations. The $G(k)$ - spectrum accounting for the corrections due to both the second and the third diagrams in (12) is displayed on Fig. 3 by the dash-dot line. On the outlined graphs, we have displayed the exponential decay of G -spectrums at given momentum k .

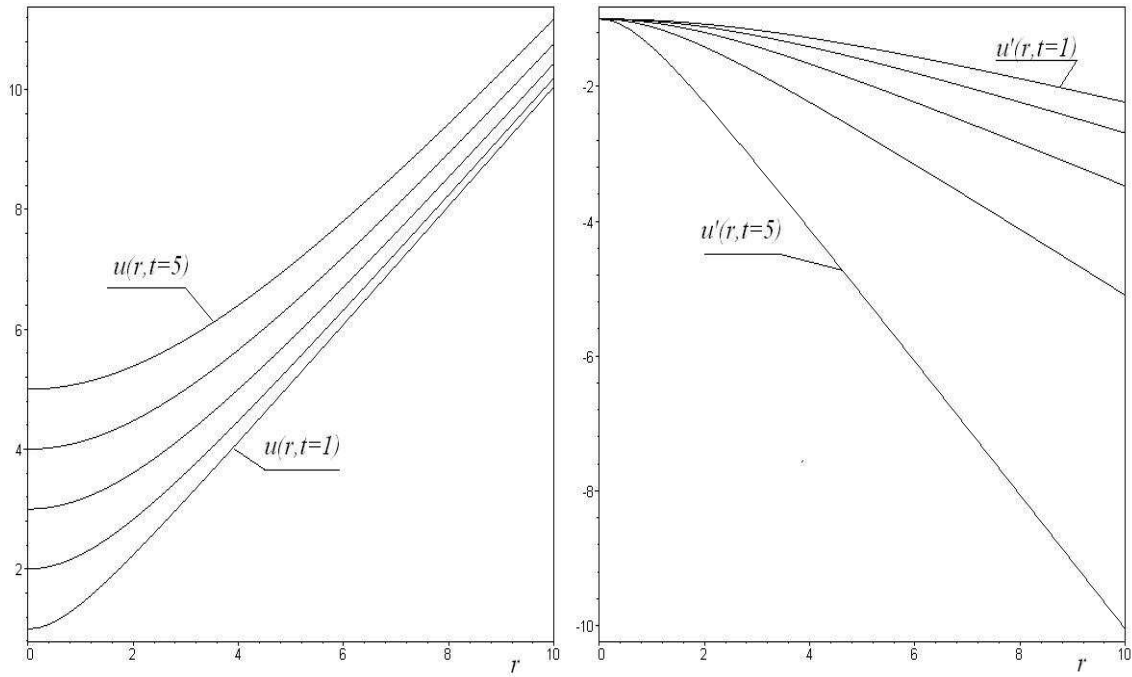


Figure 4: The radial profiles (for 5 consequent time steps) of the radially symmetric velocity field $u(r, t)$ and the auxiliary field $u'(r, t)$ which meet the saddle-point equations with respect to the high order asymptotic contributions into the Green function. These solutions correspond to the effective value $g_* \rightarrow 0$ of the coupling constant in the hydrodynamical equation and contribute the asymptotic close to the standard diffusion kernel.

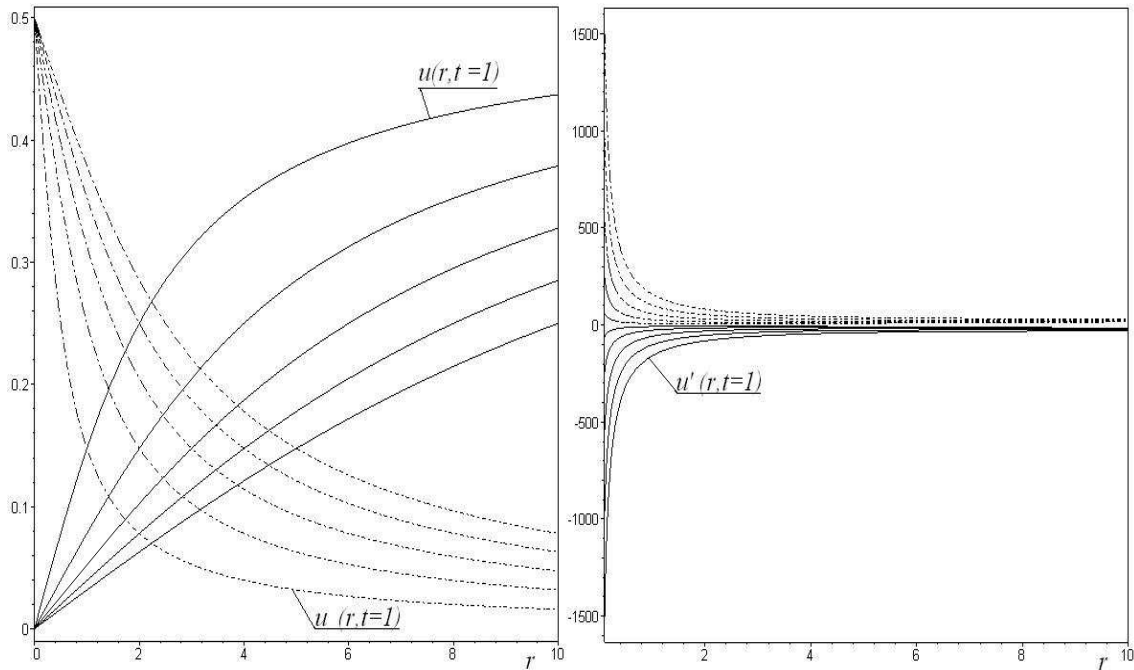


Figure 5: The radial profiles (for 5 consequent time steps) of the radially symmetric velocity field $u(r, t)$ and the auxiliary field $u'(r, t)$ which meet the saddle-point equations with respect to the high order asymptotic contributions into the Green function. The solutions correspond to the effective value $g_* \rightarrow \infty$ of the coupling constant in the hydrodynamical equation. They do not contribute into the high order asymptotic coefficients.

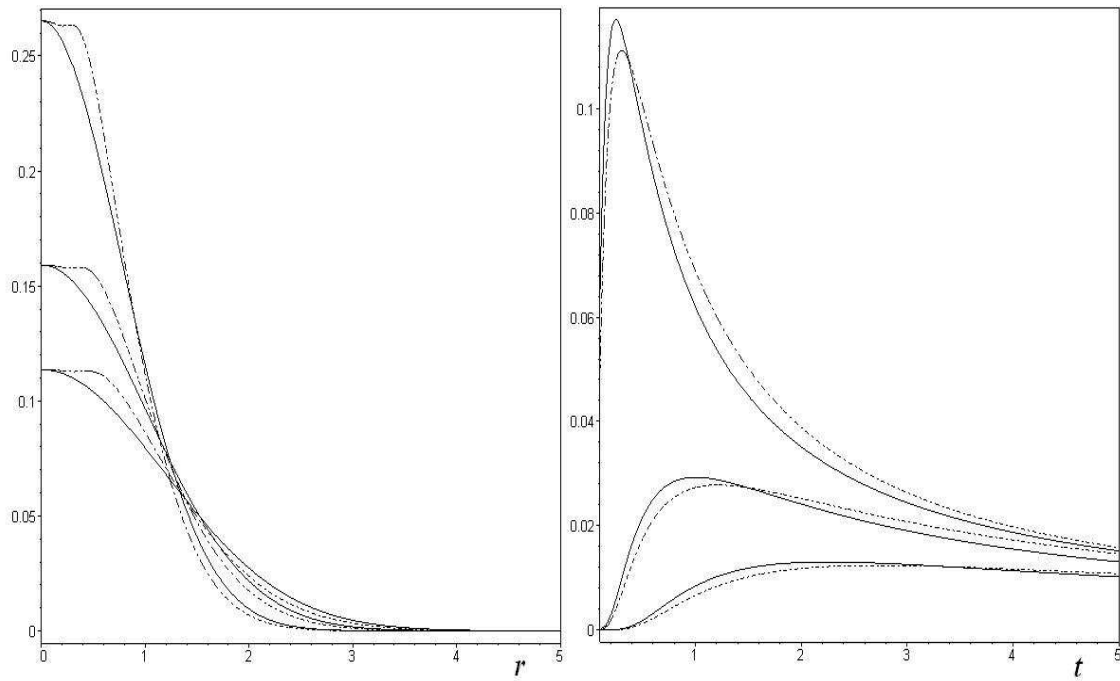


Figure 6: The profiles of standard diffusion kernel (the solid line). On the left: $G(r)$ at several consequent time steps; on the right: $G(t)$ at several distant points. The dash-dot lines present the asymptotic kernel (as $t \rightarrow t_0$) accounting for all bifurcations (up to an infinite order) of vortices.